International Journal of Modern Physics E
© World Scientific Publishing Company

arXiv:1310.6389v2 [hep-lat] 13 Feb 2014

The electromagnetic form factor of the pion: Results from the lattice

Bastian B. Brandt
Institut für theoretische Physik
Universität Regensburg, D-93040
bastian.brandt@physik.uni-regensburg.de

This review contains an overview over recent results for the electromagnetic iso-vector form factor of the pion obtained in lattice QCD with dynamical fermions. Particular attention is given to the extrapolation to the physical point and an easy assessment of the control over the main systematic effects by imposing quality criteria and an associated sign code, similar to the ones used by the FLAG working group. Also included is a brief discussion of recent developments and future challenges concerning the accurate extraction of the form factor in the lattice framework.

Keywords: Lattice QCD, Pion Electromagnetic Form Factor, Chiral Perturbation Theory

PACS numbers: 12.38.Gc, 13.40.Gp, 14.40.Be

Contents

1. Introduction 1
2. Lattice computation of the form factor 3
   2.1. Extraction of the form factor 3
   2.2. Extrapolation to the physical point 5
3. Compilation of results for form factor and charge radius 6
   3.1. Results for the form factor 6
   3.2. Extraction of the charge radius 7
4. Results at the physical point 9
5. Summary and perspectives 12

1. Introduction

Electromagnetic form factors probe the distribution of the electrically charged particles within hadrons. In experiment, they can be measured at small space-like momentum transfers, $-q^2 \equiv Q^2$, via the Q^2 dependence of elastic scattering of electrons off hadrons, for instance. Here we are interested in the electromagnetic form factor of the pion, $f_{\pi\pi}(Q^2)$, which has been measured with high accuracy in the regime of small space-like momentum transfers by the NA7 collaboration.[1]

Measurements at larger values of Q^2 have been done at CEA/Cornell,[2] DESY[3,4] (a reanalysis of the data can be found in refs.[5,6]) and more recently at JLab.[7–9]

From the theoretical point of view, the form factor is accessible analytically only in the region of large Q^2 via perturbation theory,[10–14] in contrast to the small and intermediate Q^2 regime, the realm of strong coupling. At the current level of precision the form factor from experiment at intermediate momentum transfers is well described by a simple monopole ansatz of the form

$$f_{\pi\pi}(Q^2) = \left(1 + Q^2/M^2_{\text{pole}}\right)^{-1} \tag{1}$$

where M_{pole} is the pole mass. This model is motivated by the vector pole dominance hypothesis[15–17] (VPD), assuming that the peak of the ρ-meson at time-like momentum transfers dominates the behaviour of the form factor. To bridge the gap between experimental data and the large Q^2 regime, one usually has to rely on models or effective field theory predictions.

To address the strongly coupled small Q^2 region a non-perturbative treatment is needed. A possible effective field theory framework is provided by chiral perturbation theory[18–20] (ChPT) where the Q^2 dependence of form factors can be computed order for order in the quark mass and the quark momenta. The form factor has been computed to next-to leading order (NLO) in refs.[19,20] and in refs.[21,22] to next-to-next-to leading order (NNLO) in $SU(2)$ and $SU(3)$ ChPT, respectively. However, the expansion includes unknown low energy constants (LECs) that need to be fixed to enable predictions. In addition, the energy range to which ChPT at a given order is applicable is not known *a priory* and thus has to be tested by comparison to data. Concern regarding the effective field theory framework when applied to electromagnetic form factors can be raised in regard of the tree-level coupling of the photon to vector degrees of freedom. Extensions to ChPT including vector degrees of freedom explicitly have been formulated[23,24] and the expression for the electromagnetic form factor of the pion has been computed.[25]

Numerical simulations of lattice QCD offer a method to calculate QCD observables from first principles and have been successfully applied to a number of phenomenologically relevant quantities (for a compilation see refs.[26,27]). Unfortunately, quantities related to the structure of hadrons are more difficult. Particularly problematic are form factors of baryons where the control of systematic effects such as excited state contributions[28–31] and/or finite size effects[32] is challenging (for recent reviews see refs.[33,34]). This is not surprising regarding the fact that even for $f_{\pi\pi}(Q^2)$, which is conceptually much simpler, reliable continuum extrapolated results at the physical point have become available only recently [a].

Lattice measurements of $f_{\pi\pi}(Q^2)$ have been started in the late 80's[36,37] and initially been done neglecting the effect of virtual quark loops.[38–43] The aim of this review is to provide an overview over the available lattice results for $f_{\pi\pi}(Q^2)$ and

[a]Note that the form factor can also be calculated in the framework of Dyson-Schwinger equations (see ref.[35] and references therein).

the associated charge radius, with the focus on measurements including dynamical quarks, started with the initial measurements reported in ref.[41] For an easy assessment of the control over systematic effects we will use a three-staged sign code in the spirit of ref.[26] We will start with a brief discussion of the extraction of $f_{\pi\pi}$ and the associated theoretical developments and challenges.

2. Lattice computation of the form factor

2.1. *Extraction of the form factor*

The electromagnetic form factor of the pion is defined as

$$\left\langle \pi^+(\mathbf{p}_f)|V_\mu|\pi^+(\mathbf{p}_i)\right\rangle = (p_f + p_i)_\mu \, f_{\pi\pi}(Q^2)\,, \tag{2}$$

where V_μ is the vector current, given by

$$V_\mu = \begin{cases} \frac{2}{3}\bar{u}\gamma_\mu u - \frac{1}{3}\bar{d}\gamma_\mu d & \text{for} \quad N_f = 2\,; \\ \frac{2}{3}\bar{u}\gamma_\mu u - \frac{1}{3}\bar{d}\gamma_\mu d - \frac{1}{3}\bar{s}\gamma_\mu s & \text{for} \quad N_f = 2+1 \end{cases} \tag{3}$$

and $Q^2 \equiv -(p_f - p_i)^2$ is the four-momentum transfer. At small momentum transfers the Q^2 dependence of the form factor defines the charge radius $\langle r_\pi^2\rangle$ and the curvature c_V via

$$f_{\pi\pi}(Q^2) = 1 - \frac{\langle r_\pi^2\rangle}{6}\, Q^2 - c_V\, Q^4 + \dots\,. \tag{4}$$

Starting from the VPD model, eq. (1), the charge radius and the curvature are given by $\langle r_\pi^2\rangle = 6/M_{\rm pole}^2$ and $c_V = 1/M_{\rm pole}^4$.

The matrix element on the left hand side of eq. 2 at space-like momentum transfers (time-like momentum transfers will be mentioned in section 5) can be extracted from the asymptotic time-dependence of a suitable combination of Euclidean two and three-point functions[36,38–41] in the limit of infinite temporal separation between pion creation and annihilation operators and the current insertion. At finite temporal extents one is left with contaminations from excited states. This is particularly problematic at large momentum transfers where the signal-to-noise ratio deteriorates exponentially with Euclidean time.[44] One possibility to reduce the problem is to use suitable ratios where some of the excited state contributions cancel.[37,41–43,45–51] In practice, there are two different domains where the extraction of the matrix element demands different computational methods:

(1) **Large momentum transfers:**
For lattices with periodic boundary conditions, momenta of hadrons have to be introduced by Fourier transformation, which in a finite volume leads to discrete momenta. What we denote as the regime of large momentum transfers starts around the smallest non-zero momentum transfer that can be achieved in this way (e.g. for a typical lattice with $m_\pi L = 4$ and $m_\pi = 300$ MeV $Q^2_{\rm min} =$

0.155 GeV^2). In this regime the propagating pions obtain large momenta so that the region where excited states are negligible is dominated by noise.
The standard method to overcome such a problem is to use suitable source and sink operators that increases the overlap with the groundstate, thereby leading to reduced excited state contaminations, usually at the cost of a slight growths in the noise. This can be achieved by smearing source and sink operators,[52–54] with or without blocked links[55,56] in the smearing kernel, leading to a spatially extended source which mimicks the finite extent of the quark bound state. A conventional implementation of this method allows to extract the matrix element up to $Q^2 \approx 3 - 4$ GeV^2.[41,45] A combination with all-to-all propagator methods offers the potential forfurther error reduction.[50] To be able to go to even larger momentum transfers it is necessary to use a smearing designed to improve the overlap with a boosted state.[44,57] In the first test, where the smearing parameters have been retuned for each momentum, momentum transfers as large as 7 GeV^2 could be reached.[57] Changing the kernel to an anisotropic one has proven to reduce the error bars for pion two-point functions,[44] while maintaining strong overlap with the groundstate and offers the possibility for further improvement. Other methods to reduce excited state contaminations are provided by variational[58–60] and/or summed operator insertion[28,52,61,62] techniques. However, for very large momentum transfers, larger than the inverse of the lattice spacing squared (typically $a^{-2} \sim 6$ to 16 GeV^2), large discretisation effects can appear which demand a careful extrapolation to the continuum. To overcome this problem a computationally demanding step-scaling procedure has been proposed in ref.,[57] but has not been put to a test so far.

(2) **Small momentum transfers:**
The regime below the minimal momentum transfer available by Fourier transformation can be accessed by using *partially twisted* boundary conditions[63–66] which allow to extract the form factor at arbitrary momentum transfers.[46] The phrase *partially* refers to the fact that only the boundary conditions for the quark fields in the computation of the propagators are changed. This procedure introduces an additional finite size effect which can be shown to decrease exponentially with the volume for pionic matrix elements.[64] Since in this regime the exponential decay of the signal-to-noise ratio is usually small enough to provide a signal for the whole range between source and sink, the use of stochastic estimators,[67–70] leading to a substantial error reduction for correlation functions with propagating pions,[71] enables the extraction of the form factor with high accuracy.

The main systematic effects that need to be controlled in the process of extracting the matrix element on a given ensemble are: (i) contamination from excited states; (ii) renormalisation of the vector current; (iii) full $\mathcal{O}(a)$-improvement. Whether the last two of these systematic effects apply depends on the details of the computation. Other systematic effects connected with the extrapolation to the

physical point will be discussed in the next section. Concerning the contaminations from excited states there are two types:[45,72] (a) a contribution independent of the time of the current insertion, decreasing exponentially with the temporal separation between creation and annihilation operator; (b) a contribution decreasing exponentially with the temporal difference between those and the current insertion. The latter can easily be avoided by extracting the matrix element from the region where only a single state contributes to the decay of 2 and 3-point functions. Contaminations of type (a) are more difficult to remove, but are strongly suppressed and can typically be neglected. However, with increasing precision the importance of the effect is enhanced and can possibly be of the order of the error bars in todays simulations.[72]

2.2. *Extrapolation to the physical point*

Even though most of the collaborations today have lattices very close to, or even at the physical point at their disposal, current measurements of the form factor are still restricted to unphysically large pion masses. The calculation of the form factor at the physical point thus demands a chiral extrapolation on top of the usual extrapolations to the continuum (lattice spacing $a \to 0$) and infinite volume.

The main uncertainty in the chiral extrapolation originates from the unknown exact functional form valid for a given range of pion masses. Here ChPT can provide guidance[21,22] even though the range of validity at a given order is also not known *a priory*. The full $SU(2)$ expression at NNLO is given in terms of the pion mass m_π and the pion decay constant F_π and contains five free parameters. Four of them remain in the expression for the charge radius. In contrast, at NLO it contains only one free parameter. At NLO the expression is basically linear in Q^2 (up to a mild Q^2-dependence in the function $J(Q^2)$[21]), so that its validity will be limited to the region where the curvature of the form factor is negligible, while at NNLO it contains terms up to $\mathcal{O}(Q^6)$. In practice, it turns out that for the pion masses in reach the data cannot be described consistently with ChPT to NLO.[49–51,72,73] On the other hand, the large number of free parameters at NNLO are typically not sufficiently constrained by the curvature and the pion mass dependence of the form factor alone.[49–51,72] To overcome this problem, most collaborations have used the appearance of several LECs in the expressions for different quantities for a joined chiral extrapolation, typically including the pion decay constant F_π and the pion mass m_π.[49–51,72] The region of validity of the effective theory can potentially be increased when vector degrees of freedom are added, however, the associated formula for the form factor[25] also contains a number of free parameters and has so far not been compared to lattice data.

Apart from ChPT one can also use other ansätze for the chiral extrapolation. One example is to use a chiral extrapolation for the pole mass,[45] defined via eq. (1). One should, however, keep in mind that such a chiral extrapolation depends on the validity of the VPD hypothesis. Another possibility is to use a polynomial

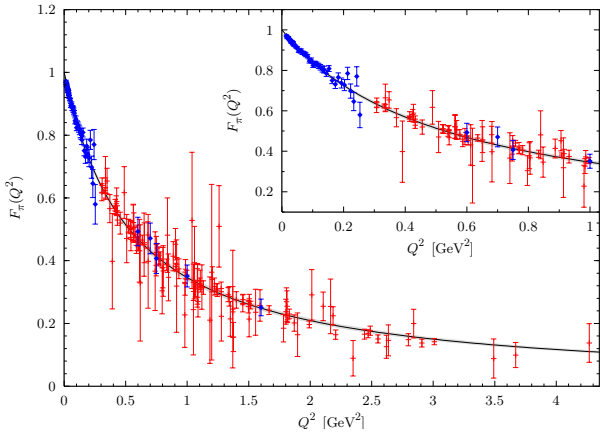


Fig. 1. Results for the electromagnetic form factor of the pion in the regime of large momentum transfers from the QCDSF/UKQCD collaboration[45] in comparison to results from experiment.[1,4,7]

extrapolation for the charge radius[49,72] which usually leads to reasonable agreement with the extrapolation via ChPT.

For the extrapolation to infinite volume it is often too expensive to perform simulations with more than one volume for each simulation point, so that one has to rely on alternative methods. One possibility is to do a finite volume study only for a few ensembles and to generalise the findings to the full set of simulation points. The extrapolation to the infinite volume limit can also be done in combination with the chiral extrapolation in the framework of ChPT. The expressions are given for Fourier momenta in ref.[74] and twisted boundary conditions in refs.[75,76] [b]. Finite volume effects for the form factor have also been studied for the ϵ-regime[78] at leading order.[79] This allows to extract the form factor on very small lattices, but relies on the assumption that higher order corrections are small.

The extrapolation to the continuum is conventionally done using a polynomial in powers of the lattice spacing a. Assuming that the theory is fully $\mathcal{O}(a)$ improved, this means that the Q^2-expansion of the form factor contains terms of the form $a^{2n}Q^{2m}$, where $n, m \in \mathbb{N}$. The terms a^2Q^2 and a^2Q^4 represent lattice artefacts for $\langle r_\pi^2 \rangle$ and c_V, respectively.

3. Compilation of results for form factor and charge radius

3.1. *Results for the form factor*

A number of collaborations have computed the form factor in the large momentum region with momentum transfers up to 4 GeV^2 using Fourier momenta[41,45–48,50,51,57,79] and twisted boundary conditions.[49] All results show good

[b]For F_π and m_π similar calculations have been done in ref.[77]

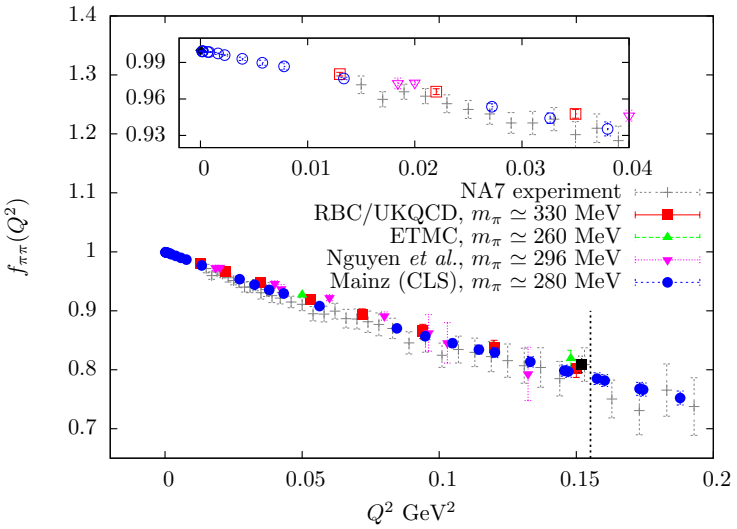


Fig. 2. Compilation of lattice results for the pion form factor[48,49,51,72] in the region of small Q^2 in comparison to the experimental results of the NA7 collaboration.[1] The black data point is the result of the RBC/UKQCD collaboration at the smallest available Q^2 from Fourier momenta and the black dashed line indicates $Q^2_{\text{min}} = 0.155$ GeV^2 the associated value for an average lattice with $m_\pi = 300$ MeV and $m_\pi\, L = 4$. The inset highlights the very small Q^2-region, displaying the potential of partially twisted boundary conditions in the approach of $Q^2 \to 0$.

agreement with a one-parameter pole ansatz, eq. (1). Newer studies with increasing accuracy, however, observe deviations from the single pole form.[50,79] So far, most of the studies in the large Q^2-regime have only been done on a single lattice spacing, so that usually a continuum extrapolation is missing. The only exception is the study by the QCDSF/UKQCD collaboration,[45] with results up to $Q^2 \lesssim 4.5$ GeV^2. They have obtained results at five different lattice spacings and various pion masses in the range of 400 to 1000 MeV, enabling a chiral and continuum extrapolation. This extrapolation, however, has been done for the pole mass directly and is thus valid only within the VPD model. As shown in figure 1 the results are in good agreement with the experimental data within the error bars.

In the small Q^2 regime, the form factor can be extracted with high precision and calculations have been done by the RBC/UKQCD,[46,48] ETM[49] and PACS-CS[51] collaborations and recently by the Mainz group.[72] A compilation of results for the form factor in this regime, including the smallest pion mass of each collaboration, is shown in figure 2. Even though at unphysically large pion masses, explaining the tendency towards larger $f_{\pi\pi}$ values, the data shows remarkable agreement with the experimental results.

3.2. *Extraction of the charge radius*

The electromagnetic charge radius of the pion, $\langle r_\pi^2 \rangle$, is defined by the expansion of the form factor given in eq. (4). Its extraction suffers from an inherent model

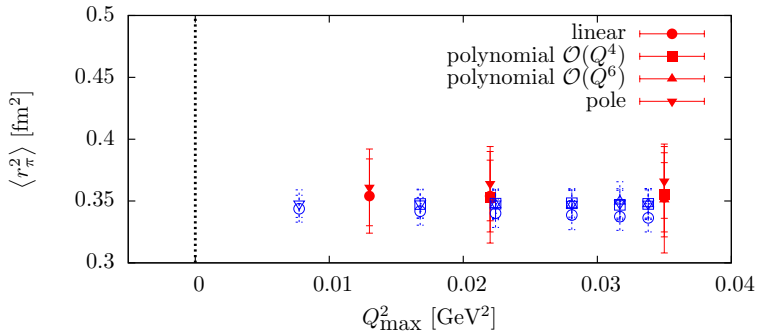


Fig. 3. Results for the form factor from the RBC/UKQCD collaboration[48] (red filled symbols) at a pion mass of 330 MeV and the Mainz group[72] (blue open symbols) at a pion mass of 325 MeV extracted from a fit to the form given in the legend.

dependence, associated with the particular ansatz for $f_{\pi\pi}(Q^2)$, unless data at very small momentum transfers is available. A comparison of the results for $\langle r_\pi^2 \rangle$ at $m_\pi \approx 330$ MeV, obtained from different functional forms including all data for the form factor up to the $Q^2_{\rm max}$ value indicated on the horizontal axis by the RBC/UKQCD collaboration[48] and of the Mainz group,[72] is shown in figure 3. The equivalence of the results from different fits below $Q^2 \approx 0.025$ GeV^2 indicates that, at the given accuracy, contributions from terms beyond the linear term are negligible. At larger momentum transfers the result from the linear fit of the Mainz group start to deviate from the other functional forms. This is not visible for the results from RBC/UKQCD, albeit possibly lost in the larger statistical uncertainties. Interestingly, the one-parameter pole fit agrees well with the unconstrained polynomials up to $Q^2 = 0.04$ GeV^2. However, this is not guaranteed to persist when data at larger Q^2 are included. In fact, data from RBC/UKQCD and also from the Mainz group indicate that the result from the one-parameter pole fit increase in this case. A similar tendency has been observed by the JLQCD/TWQCD collaboration[50] where the pole fits give smaller $\langle r_\pi^2 \rangle$ values when polynomial terms are added. In principle, a similar analysis should be done for the experimental data. However, the relatively large error bars in the low Q^2-region and the uncertainty of the normalisation at $Q^2 = 0$ of the data from the NA7-collaboration[1] makes it difficult to obtain significant results for $Q^2_{\rm max} \leq 0.1$ only.

Figure 4 contains a collection of results for the charge radius in the region of pion masses up to 600 MeV. Open symbols indicate that the result has been obtained from Fourier momenta only. The plot illustrates the good overall agreement between different collaborations. In particular, the results from the QCDSF/UKQCD collaboration rescaled with the updated lattice spacing from ref.[81] also agree well with the other lattice determinations.

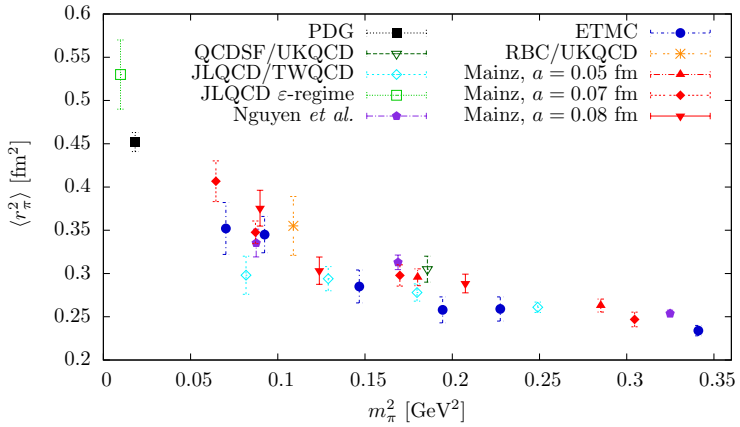


Fig. 4. Compilation of results for the charge radius from lattice QCD[45,48–51,72,79] versus the squared pion mass in physical units (here $m_\pi \leq 600$ MeV) and the experimental average quoted by the PDG.[80] Open symbols denote results extracted from form factor data with Fourier momenta only, while filled symbols represent results including data from twisted boundary conditions. The results for the QCDSF/UKQCD collaboration have been rescaled using the updated data for the lattice spacing (Sommer scale) obtained in ref.[81]

4. Results at the physical point

After the discussion of the results at non-physical pion mass we will now discuss the results for the form factor and charge radius that have been extrapolated to the physical point. To provide an indication for the control over the main systematic effects for non-experts regarding lattice QCD, we will follow the strategy of the FLAG group[26] and introduce a sign code, indicating how well a particular systematic effect is under control in an individual measurement. The criteria and systematic effects considered for the evaluation are collected in table 1 and we use the signs ✓, □and ×for full, partial and no control over the effect, respectively. The first three systematic effects and criteria have been adopted from the next update[82] of the FLAG review[26] which already contains an evaluation of the results for the charge radius (note that in the LEC section the criteria for the chiral extrapolation are those given in table 1 [c] and are different to the rest of ref.[82]). For those three criteria we agree with the assessments in the FLAG review (except for the evaluation concerning the chiral extrapolation of the QCDSF result). At this point it is important to stress that the ChPT formulae at NNLO for $\langle r_\pi^2 \rangle$ (or $f_{\pi\pi}$), F_π and m_π still has 11 to 14 free parameters (depending on the extrapolation strategy) so that some of the parameters still need to be constrained to stabilise the fits. For this different strategies have been pursued,[49–51,72] thereby introducing another systematic effect concerning the chiral extrapolation, whose impact is difficult to quantify.

[c] I would like to thank Stephan Dürr for pointing this out.

Systematic effect	abbrev.	criteria for ✓	criteria for □
Chiral extrapolation	ChE	$m_{\pi,\mathrm{min}} < 250$ MeV	$m_{\pi,\mathrm{min}} \leq 400$ MeV
Continuum extrapolation	CoE	3 or more lattice spacings$^{(i)}$	2 lattice spacings$^{(i)}$
Finite volume effects	FVE	$m_\pi\, L \gtrsim 3.7$ &/or 2 volumes$^{(ii)}$	$m_\pi\, L \gtrsim 3$
Model dependence in $\langle r_\pi^2 \rangle$ extraction	MD	at least 2 points with $Q^2 < 0.03$ GeV^2	a detailed comparison of several fit functions

Table 1. List of systematic effects evaluated for the extraction of the charge radius. If the criteria above have not been fulfilled we have attributed a '× ' sign. $^{(i)}$ We also adopt the additional criteria from the update[82] of the FLAG review: $a^2_{\mathrm{max}}/a^2_{\mathrm{min}} \geq 2$, $D(a_{\mathrm{min}}) \leq 2$ % and $\delta(a_{\mathrm{min}}) \leq 1$ for a '✓'; $a^2_{\mathrm{max}}/a^2_{\mathrm{min}} \geq 1.4$, $D(a_{\mathrm{min}}) \leq 10$ % and $\delta(a_{\mathrm{min}}) \leq 2$ for a '□ ' (see ref.,[82] section 2, for notation and details). $^{(ii)}$ The two volumes have to be at fixed other parameters and in the case of $m_\pi\, L \gtrsim 3.7$ they can be replaced by estimating the effect in ChPT instead.

Collaboration	N_f	ChE mth.	ChE	CoE	FVE	MD	$\langle r_\pi^2 \rangle$ [fm^2]
QCDSF/UKQCD[45]	2	M_{pole}	×	✓	□	×	0.509(22)(74)
ETMC[49]	2	NNLO $f_{\pi\pi}$	□	□	□	□	0.456(30)(24)
JLQCD/TWQCD[50]	2	NNLO $f_{\pi\pi}$	□	×	×	□	0.409(23)(37)
Mainz[72] (CLS)	2	NNLO $\langle r_\pi^2 \rangle$	□	✓	✓	✓	0.481(34)(13)
RBC/UKQCD[48]	2+1	NLO	□	×	✓	✓	0.418(31)
Ngyuen *et al*[51]	2+1	NNLO $\langle r_\pi^2 \rangle$	□	×	✓	✓	0.441(46)
PDG[80]		—					0.452(11)
Amendolia *et al*[1]		—					0.439(8)
BCT[21]		—					0.437(16)

Table 2. Collection of results for the electromagnetic charge radius of the pion from Lattice QCD with two[45,49,50,72] and three[48,51] dynamical quark flavours, experiment[1,80] and an analysis of the experimental data using ChPT at NNLO. 'ChE mth.' denotes the method used for the chiral extrapolation and N_f stands for the number of dynamical quarks used in the simulations ($2+1$ means two degenerate light and a heavier strange quark). The result for the QCDSF/UKQCD collaboration is the one which is obtained from the new scale determination.[81] The original result[45] was $\langle r_\pi^2 \rangle = 0.442(19)(64)$ fm^2. For the associated chiral extrapolation we have given the × sign, following the criteria listed above, in contrast to the assessment of the FLAG review ('green' flag[26,82]), since the minimal pion mass included is about 428 MeV with the new lattice spacing.

We have added the model dependence of the extraction of the charge radius as an additional systematic effect which is an issue for the extraction of charge radii in general as long as there is a gap in the form factor data to $Q^2 = 0$. In the case of $\langle r_\pi^2 \rangle$ we have seen in the last section that the form factor is basically linear below $Q^2 \approx 0.03$ GeV^2 with the present accuracy of the data, so that the residual model dependence in the extraction of $\langle r_\pi^2 \rangle$ is negligible. We have also seen that a careful extraction of $\langle r_\pi^2 \rangle$ comparing different functional forms leads to results that are compatible with the ones obtained from Q^2 values below 0.03 GeV^2 so that in this case there is at least some control over the associated systematic effect.

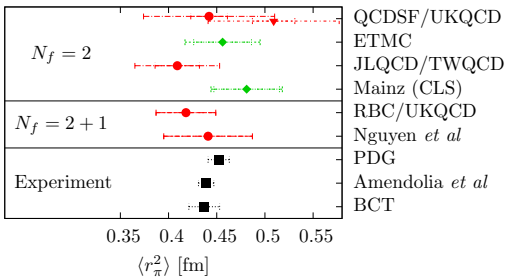


Fig. 5. Results for the pion charge radius at the physical point as given in table 2. The two different results for the QCDSF/UKQCD collaboration are the results obtained with $r_0 = 0.467$ fm (circle) and $r_0 = 0.501$ fm (triangle) (see the caption of table 2).

The available results for $\langle r_\pi^2 \rangle$ at the physical point are listed in table 2. In the assessment of systematic effects we have assumed that all collaborations fully control the effects concerning the extraction of the matrix element on a given ensemble (cf. section 2.1). The table also includes experimental results, the NA7 result[1] and the PDG average,[80] as well as a result from ChPT applied to the experimental data.[21] These results in principle share the model dependence in the extraction of $\langle r_\pi^2 \rangle$ since experimental data is only available for $Q^2 > 0.015$ GeV^2 [d]. A scatter plot of the collection of results is shown in figure 5. The measurements with at least partial control over all systematic effects, the ones from the ETMC[49] and the Mainz group,[72] are marked in green (diamonds). The plot displays the overall agreement, even though the data shows a certain spread with the more reliable results at the upper end. Note, that the remaining systematic uncertainty is mostly due to the chiral extrapolation. Future lattice calculations will have to improve on this to make a precise prediction for the charge radius at the physical point.

The chiral extrapolation for the form factor is typically done in the framework of ChPT, so that the Q^2-dependence of the form factor at the physical point can naturally be represented by its ChPT expression using the LECs from the chiral extrapolation. Figure 6 shows $f_{\pi\pi}(Q^2)$ up to $Q^2 = 0.8$ GeV^2 in ChPT at NNLO obtained by ETMC[49] and the Mainz group.[72] Note, that the results of the Mainz group only use results with $Q^2 \leq 0.077$ GeV^2 and the results from ETMC are not extrapolated to the continuum. Both curves show agreement with the experimental data. The plot also includes the Q^2-dependence (dashed lines) obtained from the VPD model with $\langle r_\pi^2 \rangle = 6/M_{\text{pole}}^2$ and the value for $\langle r_\pi^2 \rangle$ at the physical point.

For the curvature c_V less results are available in the literature, the only two being the ones from ETMC,[49] $c_V = 3.37(31)(27)$ GeV^{-4}, and JLQCD/TWQCD,[50] $c_V = 3.22(17)(36)$ GeV^{-4}. As indicated in table 2 the only one for which the main systematic effects are partially under control is the ETMC result.

[d]The data from experiment at space and time-like q^2 can also be used to derive bounds for the pion charge radius that are potentially model independent (see ref.[83]).

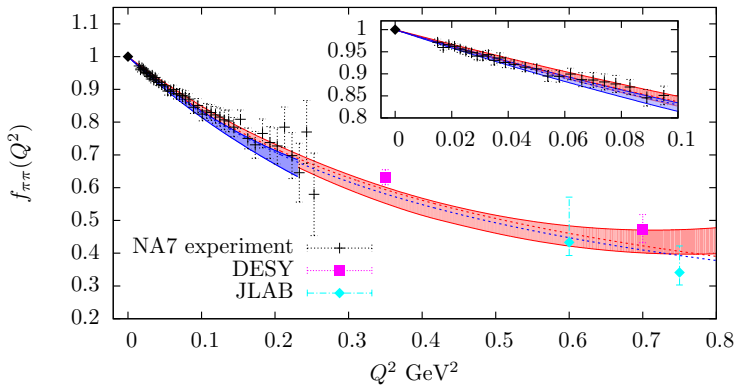


Fig. 6. Results for the Q^2-dependence of the form factor at the physical point obtained from lattice QCD (red - higher curve: ETMC;[49] blue - lower curve: Mainz[72]) using ChPT at NNLO (coloured areas) and the VPD model (dashed lines).

5. Summary and perspectives

This review contains a summary of the available measurements of the electromagnetic form factor of the pion from numerical simulations in full lattice QCD. A list of results of the charge radius has been given in table 2 and particular attention has been attributed to the indication of the control over systematic effects. Owing to partially twisted boundary conditions, lattice QCD has the unique opportunity to calculate the form factor at arbitrarily small momentum transfers, which allows for extracting the charge radius of the pion without residual model dependence. The remaining dominant systematic uncertainty is due to the chiral extrapolation, but results at the physical point, that will hopefully become available in the near future (first results have been presented at this years lattice conference by the MILC collaboration[84]), will remove this uncertainty. An accurate extraction of the charge radius, however, also demands full control over the other systematic effects. In particular, lattice simulations are usually done with degenerate light quarks and thus neglect the effects due to iso-spin breaking (for a recent review see ref.[85]). The reliable inclusion of these effects is one of the main tasks for the future.

The accurate extraction of the form factor at large momentum transfers is computationally even more challenging due to the earlier loss of the signal in the extraction of the matrix element. Clearly more work is needed to increase the control over the systematic effects and to decrease the error bars in this regime. Possible strategies have been discussed in section 2.1.

Time-like momentum transfers are not directly accessible in lattice simulations (at least for non-transition form factors) but can be accessed indirectly for the Q^2 range between the two-particle threshold ($2m_\pi$) and the inelastic threshold ($4m_\pi$), following a recent proposal.[86] Even though the method is computationally demanding first results have been presented recently.[87]

Acknowledgements: I am grateful to Andreas Jüttner for carefully going through the manuscript and illuminating discussions, Hartmut Wittig for numerous discussions on the matter, Silvano Simula for providing access to the data for the form factor of the ETM collaboration at the physical point and Jacques Bloch for information about the Dyson-Schwinger measurements.

References

1. NA7 Collaboration (S. Amendolia *et al.*), *Nucl.Phys.* **B277** (1986) 168.
2. C. Bebek, C. Brown, S. D. Holmes, R. Kline, F. Pipkin *et al.*, *Phys.Rev.* **D17** (1978) 1693.
3. H. Ackermann, T. Azemoon, W. Gabriel, H. Mertiens, H. Reich *et al.*, *Nucl.Phys.* **B137** (1978) 294.
4. P. Brauel, T. Canzler, D. Cords, R. Felst, G. Grindhammer *et al.*, *Z.Phys.* **C3** (1979) 101.
5. Jefferson Lab F(pi) Collaboration (V. Tadevosyan *et al.*), *Phys.Rev.* **C75** (2007) 055205, arXiv:nucl-ex/0607007 [nucl-ex].
6. Jefferson Lab Collaboration (G. Huber *et al.*), *Phys.Rev.* **C78** (2008) 045203, arXiv:0809.3052 [nucl-ex].
7. Jefferson Lab F(pi) Collaboration (J. Volmer *et al.*), *Phys.Rev.Lett.* **86** (2001) 1713, arXiv:nucl-ex/0010009 [nucl-ex].
8. Jefferson Lab F(pi)-2 Collaboration (T. Horn *et al.*), *Phys.Rev.Lett.* **97** (2006) 192001, arXiv:nucl-ex/0607005 [nucl-ex].
9. T. Horn, X. Qian, J. Arrington, R. Asaturyan, F. Benmokthar *et al.*, *Phys.Rev.* **C78** (2008) 058201, arXiv:0707.1794 [nucl-ex].
10. S. J. Brodsky and G. R. Farrar, *Phys.Rev.Lett.* **31** (1973) 1153.
11. S. J. Brodsky and G. R. Farrar, *Phys.Rev.* **D11** (1975) 1309.
12. G. R. Farrar and D. R. Jackson, *Phys.Rev.Lett.* **43** (1979) 246.
13. A. Efremov and A. Radyushkin, *Theor.Math.Phys.* **42** (1980) 97.
14. A. Efremov and A. Radyushkin, *Phys.Lett.* **B94** (1980) 245.
15. W. Holladay, *Phys.Rev.* **101** (1956) 1198.
16. W. R. Frazer and J. R. Fulco, *Phys.Rev.Lett.* **2** (1959) 365.
17. W. R. Frazer and J. R. Fulco, *Phys.Rev.* **117** (1960) 1609.
18. J. Gasser and H. Leutwyler, *Annals Phys.* **158** (1984) 142.
19. J. Gasser and H. Leutwyler, *Nucl.Phys.* **B250** (1985) 465.
20. J. Gasser and H. Leutwyler, *Nucl.Phys.* **B250** (1985) 517.
21. J. Bijnens, G. Colangelo and P. Talavera, *JHEP* **9805** (1998) 014, arXiv:hep-ph/9805389 [hep-ph].
22. J. Bijnens and P. Talavera, *JHEP* **0203** (2002) 046, arXiv:hep-ph/0203049 [hep-ph].
23. G. Ecker, J. Gasser, A. Pich and E. de Rafael, *Nucl.Phys.* **B321** (1989) 311.
24. G. Ecker, J. Gasser, H. Leutwyler, A. Pich and E. de Rafael, *Phys.Lett.* **B223** (1989) 425.
25. I. Rosell, J. Sanz-Cillero and A. Pich, *JHEP* **0408** (2004) 042, arXiv:hep-ph/0407240 [hep-ph].
26. G. Colangelo, S. Durr, A. Juttner, L. Lellouch, H. Leutwyler *et al.*, *Eur.Phys.J.* **C71** (2011) 1695, arXiv:1011.4408 [hep-lat].
27. J. Laiho, E. Lunghi and R. S. Van de Water, *Phys.Rev.* **D81** (2010) 034503, arXiv:0910.2928 [hep-ph].
28. S. Capitani, M. Della Morte, G. von Hippel, B. Jager, A. Juttner *et al.*, *Phys.Rev.*

D86 (2012) 074502, arXiv:1205.0180 [hep-lat].
29. J. Green, M. Engelhardt, S. Krieg, J. Negele, A. Pochinsky *et al.* (2012) arXiv:1209.1687 [hep-lat].
30. S. Capitani, M. Della Morte, G. von Hippel, B. Jager, B. Knippschild *et al.*, *PoS* **LATTICE2012** (2012) 177, arXiv:1211.1282 [hep-lat].
31. T. Bhattacharya, S. D. Cohen, R. Gupta, A. Joseph and H.-W. Lin (2013) arXiv:1306.5435 [hep-lat].
32. T. Yamazaki, Y. Aoki, T. Blum, H.-W. Lin, S. Ohta *et al.*, *Phys.Rev.* **D79** (2009) 114505, arXiv:0904.2039 [hep-lat].
33. H.-W. Lin, *PoS* **LATTICE2012** (2012) 013, arXiv:1212.6849 [hep-lat].
34. A. Walker-Loud (2013) arXiv:1304.6341 [hep-lat].
35. L. Chang, I. Cloet, C. Roberts, S. Schmidt and P. Tandy (2013) arXiv:1307.0026 [nucl-th].
36. G. Martinelli and C. T. Sachrajda, *Nucl.Phys.* **B306** (1988) 865.
37. T. Draper, R. Woloshyn, W. Wilcox and K.-F. Liu, *Nucl.Phys.* **B318** (1989) 319.
38. J. van der Heide, M. Lutterot, J. Koch and E. Laermann, *Phys.Lett.* **B566** (2003) 131, arXiv:hep-lat/0303006 [hep-lat].
39. J. van der Heide, J. Koch and E. Laermann, *Phys.Rev.* **D69** (2004) 094511, arXiv:hep-lat/0312023 [hep-lat].
40. A. M. Abdel-Rehim and R. Lewis, *Nucl.Phys.Proc.Suppl.* **140** (2005) 299, arXiv:hep-lat/0408033 [hep-lat].
41. Lattice Hadron Physics Collaboration (F. D. Bonnet, R. G. Edwards, G. T. Fleming, R. Lewis and D. G. Richards), *Phys.Rev.* **D72** (2005) 054506, arXiv:hep-lat/0411028 [hep-lat].
42. Bern-Graz-Regensburg (BGR) Collaboration (S. Capitani, C. Gattringer and C. Lang), *Phys.Rev.* **D73** (2006) 034505, arXiv:hep-lat/0511040 [hep-lat].
43. J. Hedditch, W. Kamleh, B. Lasscock, D. Leinweber, A. Williams *et al.*, *Phys.Rev.* **D75** (2007) 094504, arXiv:hep-lat/0703014 [HEP-LAT].
44. M. Della Morte, B. Jager, T. Rae and H. Wittig, *Eur.Phys.J.* **A48** (2012) 139, arXiv:1208.0189 [hep-lat].
45. QCDSF/UKQCD Collaboration (D. Brommel *et al.*), *Eur.Phys.J.* **C51** (2007) 335, arXiv:hep-lat/0608021 [hep-lat].
46. P. Boyle, J. Flynn, A. Juttner, C. Sachrajda and J. Zanotti, *JHEP* **0705** (2007) 016, arXiv:hep-lat/0703005 [HEP-LAT].
47. P.-h. J. Hsu and G. T. Fleming, *PoS* **LAT2007** (2007) 145, arXiv:0710.4538 [hep-lat].
48. P. Boyle, J. Flynn, A. Juttner, C. Kelly, H. P. de Lima *et al.*, *JHEP* **0807** (2008) 112, arXiv:0804.3971 [hep-lat].
49. ETM Collaboration (R. Frezzotti, V. Lubicz and S. Simula), *Phys.Rev.* **D79** (2009) 074506, arXiv:0812.4042 [hep-lat].
50. JLQCD Collaboration, TWQCD Collaboration (S. Aoki *et al.*), *Phys.Rev.* **D80** (2009) 034508, arXiv:0905.2465 [hep-lat].
51. O. H. Nguyen, K.-I. Ishikawa, A. Ukawa and N. Ukita, *JHEP* **1104** (2011) 122, arXiv:1102.3652 [hep-lat].
52. S. Gusken, U. Low, K. Mutter, R. Sommer, A. Patel *et al.*, *Phys.Lett.* **B227** (1989) 266.
53. C. Alexandrou, F. Jegerlehner, S. Gusken, K. Schilling and R. Sommer, *Phys.Lett.* **B256** (1991) 60.
54. UKQCD Collaboration (C. Allton *et al.*), *Phys.Rev.* **D47** (1993) 5128, arXiv:hep-lat/9303009 [hep-lat].

55. M. Teper, *Phys.Lett.* **B183** (1987) 345.
56. A. Hasenfratz and F. Knechtli, *Phys.Rev.* **D64** (2001) 034504, arXiv:hep-lat/0103029 [hep-lat].
57. H.-W. Lin and S. D. Cohen (2011) arXiv:1104.4319 [hep-lat].
58. C. Michael and I. Teasdale, *Nucl.Phys.* **B215** (1983) 433.
59. M. Luscher and U. Wolff, *Nucl.Phys.* **B339** (1990) 222.
60. B. Blossier, M. Della Morte, G. von Hippel, T. Mendes and R. Sommer, *JHEP* **0904** (2009) 094, arXiv:0902.1265 [hep-lat].
61. L. Maiani, G. Martinelli, M. Paciello and B. Taglienti, *Nucl.Phys.* **B293** (1987) 420.
62. J. Bulava, M. Donnellan and R. Sommer, *JHEP* **1201** (2012) 140, arXiv:1108.3774 [hep-lat].
63. P. F. Bedaque, *Phys.Lett.* **B593** (2004) 82, arXiv:nucl-th/0402051 [nucl-th].
64. C. Sachrajda and G. Villadoro, *Phys.Lett.* **B609** (2005) 73, arXiv:hep-lat/0411033 [hep-lat].
65. G. de Divitiis, R. Petronzio and N. Tantalo, *Phys.Lett.* **B595** (2004) 408, arXiv:hep-lat/0405002 [hep-lat].
66. UKQCD Collaboration (J. Flynn, A. Juttner and C. Sachrajda), *Phys.Lett.* **B632** (2006) 313, arXiv:hep-lat/0506016 [hep-lat].
67. S. Bernardson, P. McCarty and C. Thron, *Comput.Phys.Commun.* **78** (1993) 256.
68. S.-J. Dong and K.-F. Liu, *Phys.Lett.* **B328** (1994) 130, arXiv:hep-lat/9308015 [hep-lat].
69. UKQCD Collaboration (M. Foster and C. Michael), *Phys.Rev.* **D59** (1999) 074503, arXiv:hep-lat/9810021 [hep-lat].
70. UKQCD Collaboration (C. McNeile and C. Michael), *Phys.Rev.* **D73** (2006) 074506, arXiv:hep-lat/0603007 [hep-lat].
71. P. Boyle, A. Juttner, C. Kelly and R. Kenway, *JHEP* **0808** (2008) 086, arXiv:0804.1501 [hep-lat].
72. B. B. Brandt, A. Juttner and H. Wittig (2013) arXiv:1306.2916 [hep-lat].
73. B. B. Brandt, A. Juttner and H. Wittig (2011) arXiv:1109.0196 [hep-lat].
74. B. Borasoy and R. Lewis, *Phys.Rev.* **D71** (2005) 014033, arXiv:hep-lat/0410042 [hep-lat].
75. F.-J. Jiang and B. Tiburzi, *Phys.Lett.* **B645** (2007) 314, arXiv:hep-lat/0610103 [hep-lat].
76. F.-J. Jiang and B. C. Tiburzi, *Phys.Rev.* **D78** (2008) 037501, arXiv:0806.4371 [hep-lat].
77. G. Colangelo, S. Durr and C. Haefeli, *Nucl.Phys.* **B721** (2005) 136, arXiv:hep-lat/0503014 [hep-lat].
78. J. Gasser and H. Leutwyler, *Phys.Lett.* **B184** (1987) 83.
79. JLQCD Collaboration (H. Fukaya *et al.*), *PoS* **LATTICE2012** (2012) 198, arXiv:1211.0743 [hep-lat].
80. Particle Data Group Collaboration (K. Nakamura *et al.*), *J.Phys.* **G37** (2010) 075021.
81. G. Bali, P. Bruns, S. Collins, M. Deka, B. Glasle *et al.*, *Nucl.Phys.* **B866** (2013) 1, arXiv:1206.7034 [hep-lat].
82. *http://itpwiki.unibe.ch/flag* .
83. B. Ananthanarayan, I. Caprini, D. Das and I. Sentitemsu Imsong, *Eur.Phys.J.* **C73** (2013) 2520, arXiv:1302.6373 [hep-ph].
84. J. Koponen, Talk presented at conference 'Lattice 2013' .
85. A. Portelli (2013) arXiv:1307.6056 [hep-lat].
86. H. B. Meyer, *Phys.Rev.Lett.* **107** (2011) 072002, arXiv:1105.1892 [hep-lat].
87. X. Feng, Poster presentation at conference 'Lattice 2013' .